Transport properties of TMO interfaces

Monteiro, A. M.R.V.L.; Caviglia, A. D.; Reyren, N.

DOI
10.1007/978-3-319-74989-1_3

Publication date
2018

Document Version
Final published version

Published in
Springer Series in Materials Science

Chapter 3
Transport Properties of TMO Interfaces

A. M. R. V. L. Monteiro, A. D. Caviglia and N. Reyren

Abstract Phenomena that are absent of bulk TMO compounds can emerge at their interfaces when they are grown on top of each-other. A prototypical example of such emerging states is found at the $LaAlO_3/SrTiO_3$ interface, which also attracted most of the initial interest for this new field of research (in the TMO context). Here we review some properties of this peculiar interface as investigated by transport measurements allowing the studies of different effects such as magnetism, superconductivity or Rashba effect; hence indirectly accessing the band structures studied by the methods presented in the rest of the book.

3.1 Introduction

Electronic dc transport is a fundamental tool for the study of TMO interfaces, providing complementary information to spectroscopic techniques. We will illustrate this fact in the case of the $LaAlO_3$ films grown on top of (0 0 1)-oriented TiO_2-terminated $SrTiO_3$ substrate. A two-dimensional system (2DES) is found at this particular interface. Electrostatic field effect experiments have proven to be particularly valuable as they allowed tuning of the carrier density in a very sensitive region of the phase diagram in which TMO interfaces undergo quantum phase transitions (insulator to metal/superconductor) accompanied by various changes in electronic properties. Here we will discuss changes in (1) mobility and carrier localization, (2) spin-orbit

A. M. R. V. L. Monteiro (✉) · A. D. Caviglia
Kavli Institute of Nanoscience Delft University of Technology,
Lorentzweg 1, 2628 CJ Delft, The Netherlands
e-mail: A.M.Monteiro@tudelft.nl

A. D. Caviglia
e-mail: A.Caviglia@tudelft.nl

N. Reyren
Unité Mixte de Physique, CNRS, Thales, Univ. Paris-Sud,
Université Paris-Saclay,
91767 Palaiseau, France
e-mail: nicolas.reyren@cnrs-thales.fr

C. Cancellieri and V. Strocov (eds.), *Spectroscopy of Complex Oxide Interfaces*, Springer Series in Materials Science 266,
https://doi.org/10.1007/978-3-319-74989-1_3

coupling, (3) capacitance, (4) polar order and domain wall conductivity and (5) thermopower. Field effect on superconductivity is discussed in a dedicated section. The purpose of this discussion is to highlight some of the insight on oxide interfaces acquired during the past 10 years through transport and field effect experiments.

In 2006, 2 years after the discovery of the conducting $LaAlO_3/SrTiO_3$ (LAO/STO) interfaces, Thiel et al. reported the first results on the effects of electrostatic gating in this system [1]. It was shown that (a) a critical thickness of 4 u.c. of LAO exists for conductivity and (b) a 3 u.c. sample can be made conducting (and reversibly turned insulating) at room temperature by means of the electrostatic field effect, using a back gate geometry (the STO substrate acts as a gate dielectric). The same approach was used to determine the influence of gating on the superconducting properties. In 2008, it was demonstrated that the electrostatic field effect can lead to an on/off switching of superconductivity, uncovering a complex phase diagram with a non-superconducting phase, a quantum critical point, underdoped and overdoped 2D superconducting regions [2].

Mobility and carrier localization. C. Bell et al. showed that gating in LAO/STO leads to a large change in carrier mobility [3], measured through Hall effect experiments. In the underdoped region of the phase diagram a mobility of the order $10^2\,\mathrm{cm}^2/\mathrm{Vs}$ is observed. Its magnitude continuously increases up to several $10^3\,\mathrm{cm}^2/\mathrm{Vs}$ as the system is brought into the overdoped region by means of electrostatic gating. It was argued that this effect is related to a variation in the spatial confinement of the electronic wave functions in the out-of-plane direction. Around the same time, carrier localization mechanisms were considered. In the non-superconducting state it was shown that carriers undergo weak localization, evidenced by a negative quantum correction to the conductivity, correction which is suppressed by magnetic fields, meaning that a negative magnetoresistance is observed.

Spin-orbit coupling. In 2010 it was shown by means of magnetotransport experiments, that spin-orbit coupling undergoes large changes throughout the phase diagram of the system [4]. As the system enters a gate voltage range corresponding to the underdoped superconducting regime, a steep rise in spin-orbit coupling is observed, leading to a spin-splitting of the Fermi surface up to $\sim 10\,\mathrm{meV}$. A similar correlation between spin-orbit coupling and superconductivity is observed also in the overdoped regime [5]. The magnitude of the spin splitting is comparable to the Fermi energy, indicating that spin-orbit coupling is a dominant energy scale of the system. This leads to various interesting magnetotransport effect, including conductance oscillations with respect to the angle between the magnetic field and the current vector [6] and a complex evolution of the Shubnikov-de Haas oscillations with gating [7, 8]. More recently, Boltzmann transport calculations have shown that spin-orbit-induced modifications of the Fermi surface can also account for the large in-plane magnetoresistance observed in LAO/STO [9].

Capacitance enhancement. The electrostatic field-effect can be used in order to bring the electron system on the verge of strong carrier localization. In this regime, it was shown that top-gated LAO/STO exhibits a very large enhancement of capacitance [10], attributed to a negative electron compressibility, arising from correlation or disorder effects. It was argued that these effects offer a route for reducing operating voltages in field effect transistors.

Lattice effects: polar order and domain wall conductivity. Further insight into gating and electron localization in LAO/STO was acquired in 2013 by Rössle et al. [11]. Using ellipsometry and x-ray diffraction experiments, they showed that a 1 μm thick region of the STO substrate, undergoes a polar structural phase transition at temperatures below 50 K under the application of a negative gate voltage. This was evidenced by the electric-field induced splitting of an infrared active phonon mode observed only in the tetragonal phase of STO, representing antiphase rotations of oxygen octahedra. A second evidence presented was the electric-field induced satellite peaks observed around a specific Bragg x-ray reflection, representing spatial modulations of the polar order. It was argued that the electron localization observed at LAO/STO in field effect experiments is either influenced or even induced by the polar order: this phase transition strongly reduces the lattice polarizability of STO at the interfaces. This in turns reduces the dielectric screening and enhances the effect of disorder leading to a tighter confinement and a decrease in mobility. Additional indications for polar order in LAO/STO, in the absence of gating, are provided by electron microscopy experiments [12, 13]. The data points at polar order developing even at room temperature at much sharper (atomic) length scales, involving a combination of octahedral rotation and polar displacements in both LAO and STO. The effect of electrostatic gating on these short-scale atomic displacements remains to be investigated.

A second class of lattice effects relevant to transport and gating experiments in LAO/STO pertains to the tetragonal ferroelastic domains formed below 105 K. By means of a scanning single electron transistor technique, Honig et al. [14] demonstrated that the electrostatic landscape of LAO/STO is a direct map of the tetragonal domains of STO, with the local potential exhibiting $\sim$1 mV steps at the domain boundaries between in-plane and out-of-plane oriented domains. As the LAO/STO interface is gated, these domains move by $\sim$1 μm/V driven by either anisotropic electrostriction or direct coupling to polar walls. Importantly for transport experiments, Kalisky et al. [15] have shown, using a scanning magnetometry technique, that these domain boundaries constitute enhanced conduction paths. This can be understood as a combined effect of enhanced carrier density and mobility at the domain walls. Motivated by these findings, the investigation of nanoscale properties of LAO/STO remains to this date a frontier area of research that is discussed below in a separate section.

Thermopower. In 2010 Pallecchi et al. [16] considered the Seebeck effect of LAO/STO under the application of gating down to 77 K. The data is consistent with a tightly confined layer with a 2D density of states. Electrostatic gating was found to change the carrier density as well as the width of the confinement. More recently, the same authors have considered thermopower at low temperature and at gating fields on the verge of carrier depletion [17]. They observe a remarkably high thermopower (10^5 μV/K) oscillating as a function of the gate voltage, attributed to a periodic density of states arising from localized states.

3.2 Evidence for Multi-band Conduction from Magnetotransport

At high carrier densities (several $10^{13}\,\mathrm{cm}^{-2}$), magnetotransport at the LAO/STO interface displays a complex evolution in magnetic field, which has been attributed to the presence and occupation of several electronic bands [3, 7, 18–20]. Evidence of the existence of several bands has also been provided by Nernst effect measurements [21]. A growing body of theoretical models have been proposed to explain the multiband transport, making room to accommodate for its peculiar gate voltage dependence [3, 21–25]. The electron spatial distribution in the confinement potential has been a key ingredient, providing an explanation for the existence of bands with different mobilities, accessible at different electrostatic doping levels set by the application of a gate-voltage.

3.2.1 Anisotropic Magnetotransport

From an extensive list of exotic properties, one of the most surprising experimental observations is the peculiar anisotropy of magnetotransport under externally applied magnetic fields of large magnitude. When the field is applied in the plane of the 2DES, a large negative magnetoresistance is observed, showing a dramatic bell-shaped drop in resistance with respect to its zero-field value [9, 25, 26]. This negative magnetoresistance is extremely sensitive to the angle of the applied magnetic field, vanishing when the field is slightly tilted out of the plane. Furthermore, a strong, approximately six-fold, anisotropy in transport is observed with respect to the angle of the applied field within the plane of the 2DES [25].

At low temperatures, Shubnikov-de Haas oscillations in the longitudinal resistivity have been observed [7, 20], from which the extracted carrier density is one order of magnitude smaller than that extracted from the Hall effect. To date, the origin of this discrepancy is missing a clear explanation. At small magnetic fields applied perpendicularly to the plane of the 2DES, the magnetoresistance gradually changes sign as a function of gate-voltage from negative (WL) to positive (WAL) [4, 6], originating from spin-orbit coupling with a rather large energy scale. Interestingly enough, superconductivity was shown to emerge at the same gate-voltage that strong spin-orbit coupling sets in [4, 5].

3.2.2 Universal Lifshitz Transition

For samples displaying high-mobility, a simple yet effective model was put forward to explain the observed transport. Experiments have shown [24] that, for this type of samples, there is a critical carrier density below which the Hall voltages are linear in magnetic field, indicating that transport follows a single-band behavior. Above this critical density, Hall curves become non-linear, which is consistent with a two-band transport. This transition is observed to occur at a critical carrier density of $\sim 1.6 \times 10^{13}\,\mathrm{cm}^{-2}$ for several samples with different thicknesses and mobilities. This apparent universality hints that the observed transition is not disorder-driven [27], but instead has its origin in intrinsic properties of the 2DES.

This scenario predicts that the critical density corresponds to a Lifshitz transition between the population of a single, light along the conduction plane, d_{XY} band and the additional population of two heavy bands: the d_{XZ} and the d_{YZ}. The reason for the difference in their mobilities can be understood from a simple geometrical argument: both the d_{XZ} and d_{YZ} bands have one pair of lobes pointing out-of-plane, while both lobes of the d_{XY} are in plane, shifting this band to a lower energy. Gate-dependent angle-resolved photoemission spectroscopy measurements recently corroborated this scenario [28]. This band picture provides an elegant explanation for the sudden appearance of spin-orbit interactions as a function of gate-voltage. Spin-orbit interactions should be most prominent where the bands are degenerate, which corresponds exactly to the energy where the heavy bands start being populated, i.e., the Lifshitz transition. In turn, the influence of Rashba spin-orbit coupling is also peaked at the Lifshitz point, because it is directly proportional to the atomic spin-orbit coupling. The resulting band structure, introduced by Ruhman et al. [29], has been pivotal to explain various magnetotransport phenomena [6, 9, 30, 31].

3.3 Ground State of the $LaAlO_3/SrTiO_3$: Superconductivity and Magnetism

In 2007, shortly after the discovery of the 2DES at the LAO/STO interface, magnetic effects were reported in this system, based on the observation of hysteretic magnetoresistances at 0.3 K [32]. This was especially exciting, as magnetism is not present in any of the bulk components, revealing new states emerging from "boring band insulators" by their combination. At the same time, it was discovered that the 2DES is also superconducting below about 0.2 K [33]. Moreover, these measurements were compatible with a two-dimensional (2D) superconducting system, with a peculiar type of transition, as it was later confirmed by other experiments [2, 5, 34]. Both phenomena being thought to be antagonist, and indeed not being observed in the same samples in these first years, it triggered a debate about the "true nature" of the ground state. Possible explanations rely on the presence of oxygen vacancies: On one hand, it was suggested that the superconductivity state is obtained when the carrier concentration is increased due to their presences; on the other hand it was also suggested that the same vacancies were responsible for titanium polarization. Several years later, coexistence of superconductivity and magnetism was reported [35, 36], but some techniques indicate that superconductivity and magnetism might be spatially separated [37], or occurring in different electronic bands [38]. Due to the difficulties inherent to the pulsed laser deposition (note however that superconducting samples have also been fabricated using growth by molecular beam epitaxy [39]), the extreme sensitivity of the $SrTiO_3$ to oxygen defects, and the variation of $SrTiO_3$ substrate qualities (number of defects, chemical content, etc.), different groups might conclude differently simply because they have different samples.

This section will focus on three topics, first on magnetism, then on superconductivity and its two-dimensional nature, and finally on the modulation of the LAO/STO properties by electrostatic field effect.

The first indications of “magnetic effects” [32] were relying on hysteresis in the magnetoresistance curves (see Fig. 3.1a). The interpretation of the curves (which were also depending on the sweep rate of the magnetization) could not give a clear picture of the mechanisms at play. Magnetoresistance and Hall effect remained a technique of investigation of the magnetic effect, and qualitative behavior could be reproduced considering two conducting bands in parallel, one of them containing magnetic impurities [38]. Other effects related to the Rashba effect at the interface might be responsible for magnetic-like effects [40]. Macroscopic magnetic measurements were also performed, but the magnetic volume and the associated moments being so weak or diluted, totalizing a few $\mathrm{nA\,m^2}$ at most, their interpretation must be extremely cautious [35, 41]. Alternatively, x-ray magnetic circular dichroism at the Ti $L_{2,3}$-edge (the magnetism being potentially found in the 3d band of Ti [42], even though it was also predicted to occur at the $LaAlO_3$ surface [43]) gives more direct evidence of “intrinsic” (not related to impurities) magnetism situated at the interface, or at least close to it. Some groups reported [44] the observation of such dichroism, other did not find any (see e.g. [45] or supplementary of [46]). It was also reported that oxygen vacancies seem to play a major role in the observation of the Ti dichroic signal in LAO/STO [47]. Local probe, precisely a micro-SQUID, allowed to observe localized and disconnected dipole patches ($<3\,\mu\mathrm{m}$ and $\sim 10^7 \mu_B$) [37] (Fig. 3.1b) situated probably near the interface and sensitive to the tip pressure [48]. This last observation suggested a role of strain related to defects and to step edges. Magnetic force microscopy may have also revealed some magnetic patches [49]. Finally, LAO/STO has been used as an electrode in a magnetic tunnel junction with Co as second electrode [50]. The tunnel magnetoresistance signal changes with gate voltage, suggesting a connection with the 2DES, but results are varying with thermal cycling, pointing again to a phenomenon related to defects or domain walls appearing at the $SrTiO_3$ cubic-tetragonal structural phase transition at about 105 K [51]. It has also been suggested that the ground state could be a long-wavelength spiral [52]. The magnetic effects at the LAO/STO interface are hence still matter of research to understand the phenomenon in more details.

The $SrTiO_3$ is known to be superconducting in bulk systems when it is oxygen deficient [53, 54] or if it is doped by substitution of Ti by Nb or Sr by La [55]. It was hence natural to think that chemical doping could explain this observation. Interestingly, the growth of superconducting very thin films (<10 nm) of cation-doped $SrTiO_3$, either by La or Nb, was failing until a new strategy was adopted: Growing a “delta-doped” $SrTiO_3$ avoids band-bending effects at the surface and hence allowed the fabrication of extremely thin (5.5 nm) layers of doped $SrTiO_3$ which exhibit very similar

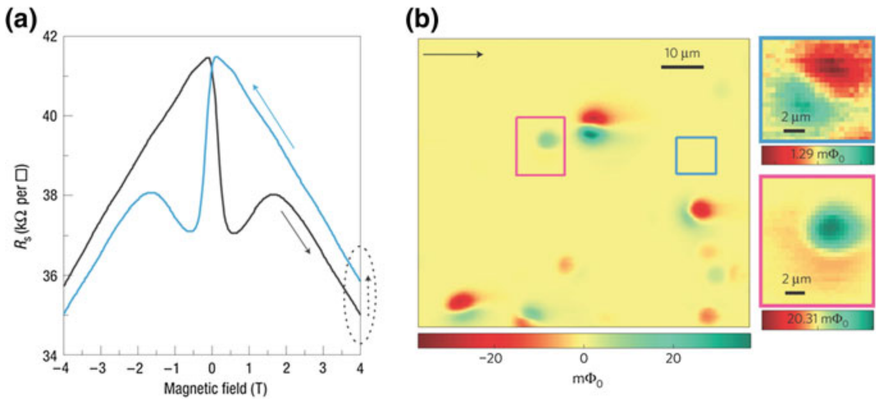

Fig. 3.1 Magnetic effects at the LAO/STO interface. **a** First hints of magnetic properties were revealed by hysteretic magneto-resistance curves at low temperature [32]. **b** Later, local SQUID measurements exposed the presence of local dipoles totalizing typically 10^7 Bohr magnetons [37]

superconducting properties than the LAO/STO system [56]. When $LaAlO_3$ is grown on top of $SrTiO_3$, similar band-bending might occur, but probably not strong enough to insure conductivity due to the differences in workfunctions only [57]. For bulk Nb-doped $SrTiO_3$, the superconductivity shows two gaps [58], but this was not observed in the LAO/STO system [59]. The coupling mechanism could be a rather conventional BCS electron-phonon, despite the low carrier density. Interestingly, on the other hand, a pseudogap temperature has also been found, indicating that the 2D superconductivity at the LAO/STO interface might share some ingredients with high-temperature superconductors [59, 60].

The two-dimensional character of the superconductivity in LAO/STO manifests itself in several aspects. We detail two of them: the resistive transition in temperature and the anisotropies of the critical magnetic fields. For 2D materials where a Berezinskii-Kosterlitz-Thouless (BKT) transition is expected, a finite resistance appears at temperature at which the thermally activated vortex-antivortex pairs unbind. In the LAO/STO case, a more complex case of the melting of a vortex-antivortex lattice could replace the conventional BKT mechanism, and is indeed quantitatively agreeing with observations [33]. The resistance as a function of temperature follows a characteristic law close to the BKT transition temperature T_{BKT} and the current-voltage curves exhibit a power-law $V = I^a$, the a coefficient taking the value 3 at T_{BKT}, as it was observed now is several groups [2, 33, 61]. Deviations from these laws are associated with finite size effects [62]. A somewhat more direct evidence for the 2D nature of the superconducting state is the anisotropy of the critical magnetic fields [34]: Applying the field in-plane or out-of-plane leads to markedly different effect. Considering a superconductor with a magnetic field applied in-plane, if its thickness is lower than its coherence length, the wave function amplitude cannot vary over it, and hence the superconductivity is not destroyed before the field-associated energy goes beyond the pairing energy. This happens in

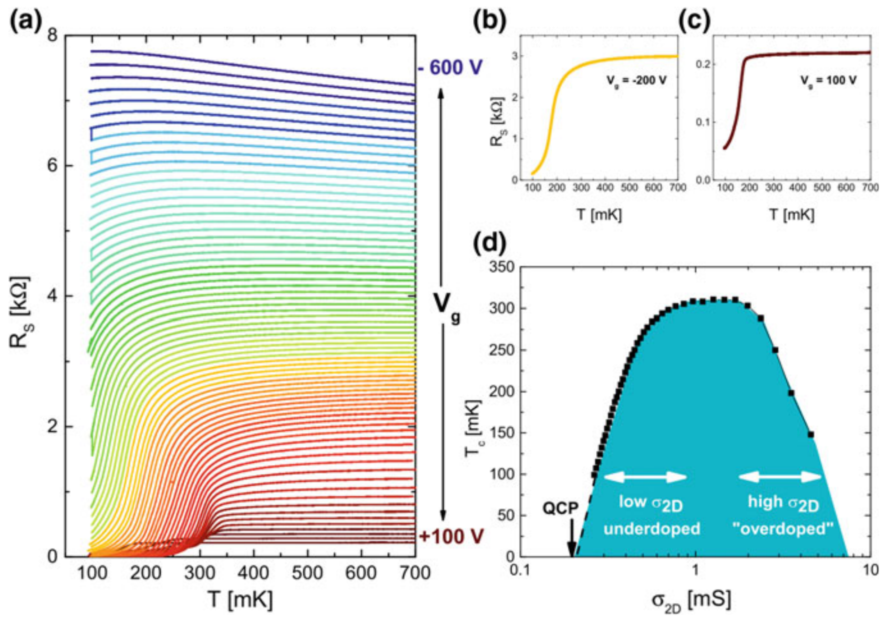

Fig. 3.2 Superconductivity and its modulation in the LAO/STO system: **a** Resistive transition as a function of the gate voltage, displaying a remarkable tunability and a superconductivity-insulator transition near the lowest doping; **b**, **c** zoom on the high concentration curves; **d** resulting phase diagram with the superconducting T_c dome as a function of the normal state sheet conductance, which reflects the carrier concentration. Figure from [66]

BCS systems at the Clogston-Chandrasekhar paramagnetic limit [63, 64] given by $\mu_0 H_{CC} = \Delta(0)/(\sqrt{2}\mu_B)$, where $\mu_0 H_{CC}$ is the applied field, $\Delta(0)$ is the gap energy at $T = 0$, μ_B is the Bohr magnetron and a gyomagnetic ratio of 2 is assumed. It has been observed that this limit is overcome by a factor 5 [5, 34]. This is an extremely strong indication of the 2D nature of the superconductivity in LAO/STO and it also reveals that spin-orbit effects or other corrections such Fulde-Ferrell-Larkin-Ovchinikov type of condensate [65] must be taken into account for a precise quantitative description of the observed critical fields.

Owing to the very low carrier concentration (of the order of $10^{13}\,\mathrm{cm}^{-2}$) of the 2DES, the extremely large dielectric constant ($\sim 10^4\,\varepsilon_0$) of the $SrTiO_3$ substrate at low temperature, and its two dimensional nature, electrostatic field effect using the $SrTiO_3$ substrate as a gate dielectric is very efficient to modulate the properties of LAO/STO. In particular, it has been possible to tune the superconducting state and reveal a dome-like shape of the critical temperature as a function of the gate voltage, or the carrier concentration [2, 60, 67]. "Top gates" (without $SrTiO_3$) lead to similar properties, even though the mechanism is cleaner, it is harder to realize [67–69]. Side gates taking again advantage of the huge dielectric constant of $SrTiO_3$ have also been used [70, 71]. Finally, it is noteworthy that the adsorbates at the surface of $LaAlO_3$ influence the properties of the 2DES [72]. Whatever the doping technique, a superconducting dome is found: the critical temperature first increases with the carrier number, it culminates at about 0.3 K and then reduces as the carrier number is further increased, as visible in Fig. 3.2. At the low concentration edge of the dome, a quantum critical point (QCP) is found, corresponding to a superconductor to insulator transition [2, 66]. Explaining this dome shape is rather complicated as many parameters are at play. First the volume carrier density does not scale linearly with the areal carrier density, which is the quantity that is modulated with gate voltages (without mentioning extra difficulties stemming from trapped states in $SrTiO_3$ [73]): Indeed due to the strong field-dependence of the $SrTiO_3$ dielectric constant, and the electrical potential well shape, the 2DES can actually expand as carrier concentration is reduced! Second, as the areal carrier concentration is increased, different conduction bands get populated, and associated to the different bands is a more or less strong Rashba spin-orbit coupling. As mentioned above, as the Rashba coefficient strongly increases (several folds), the superconducting transition appears and culminates [4]. The correlation between Rashba and superconductivity might be more than coincidental…

The ground state properties of LAO/STO are hence still a matter of active research! But whatever the nature of the "true" ground state, the superconductivity that can be modulated by gate voltage or by geometrical constriction establishes a very unique test system to understand two dimensional, or even one-dimensional superconductivity, and, who knows, even help to uncover the mysteries of high temperature superconductivity.

3.4 Nanopatterning

Patterning of the interfacial 2DES is crucial to the realization of functional electrical devices. When compared to their semiconductor counterparts, where the 2DES is typically buried hundreds of nanometers below the surface, the 2DES at the LAO/STO interface offers the exciting possibility of extremely reduced dimensions, since it lives only a few nanometers below the surface. However, producing high quality nanoscale structures at the LAO/STO interface has proven challenging due to inherent stoichiometric and structural intricacies associated with complex oxides [74]. Here, we make a brief overview of the main approaches to patterning LAO/STO and the progress in creating functional devices in this system.

Conventional photo- and e-beam lithographic techniques have been extensively used to laterally define structures by locally controlling the thickness of the crystalline LAO layer [75]. The STO substrate is patterned prior to the LAO thin film deposition and, after development, an amorphous LAO layer is deposited. After lift-off, the STO substrate is cleared in the areas protected by the resist, thus yielding conducting regions upon epitaxial LAO growth. The areas covered by the amorphous layer remain insulating. Figure 3.3b shows a microbridge realized by means of this technique. In certain cases, to ensure that resist residue does not disrupt the

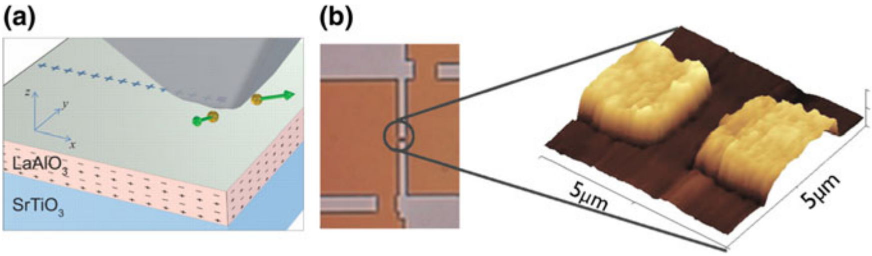

Fig. 3.3 Nanopatterning techniques. **a** AFM tip moving left to right above a 3 u.c. LAO/STO interface, locally changing the charge state of the surface creating a conducting wire. From [77]. **b** Atomic force microscope image of an 800 nm wide bridge. Polycrystalline/amorphous LAO, grown on the amorphous STO, has a lighter color, while the epitaxial LAO has a darker one. The 2DES is created only below the epitaxial LAO. From [76]

conducting interface in the device region, 2 unit cells of LAO are first deposited epitaxially over the entire substrate, after which the process described above is performed. By using this patterning method, conducting features as small as 500 nm have been achieved with e-beam lithography [76].

Conducting features down to just 2 nm have been realized through the direct atomic force microscope (AFM) writing technique [78]. A sub-critical-thickness (3 u.c.) LAO thin film is deposited on the entire substrate, which can be locally and reversibly switched between a conducting and insulating state by applying a positive or negative voltage to the AFM tip, respectively (see Fig. 3.3a). The most widely recognized mechanism of formation for this metastable conductive state is the local modification of the surface charge [79] through voltage-mediated addition and removal of water in the form of OH and H^+ [80].

3.5 Other Paths of Exploration

3.5.1 Spintronics

Spintronics is an alternative information scheme which uses the spin of the carriers, rather than their charge. Devices will require the injection, transport, modulation and detection of spin currents. The LAO/STO could be an interesting platform to test spintronics ideas, particularly owing to the possibility to modulate the Rashba effect (acting on the spin current) in this system of relatively large mobility. A first step towards such possibilities has been indirectly demonstrated with the spin injection at the LAO/STO interface from a conventional ferromagnetic metal electrode [81, 82]. Again, the behavior of the 2DES at the LAO/STO interface seems to be slightly different from what is observed in Nb-doped $SrTiO_3$ [83, 84], but the field of research is still at its infancy for $SrTiO_3$-based systems and further studies will be needed to get rid of the measurement problems and artifacts related to the tunnel barriers. In particular, so-called "non-local" measurements still need to be realized in order to directly measure the spin diffusion length.

Another interesting use of the LAO/STO system in spintronics is related to the spin to charge current conversions. Due to the Rashba interaction, spin and momentum are coupled, meaning that a charge current can imply a spin accumulation, and reciprocally. This spin accumulation can relax in a nearby material and hence produces a spin current. If a ferromagnet is placed in contact, the LAO/STO 2DES will produce a spin-torque on its magnetization, as it was first observed in 2014 [40]. The reciprocal effect (spin pumping from a ferromagnet into the 2DES, creating a charge current) has been observed recently, and very interestingly, a gate voltage can strongly modulate the amplitude (reaching values larger than what can be found in metal multilayers) and even the sign of the effect can be changed [85].

The LAO/STO system is hence showing very interesting properties in the framework of the spintronics, and its study will surely lead to other remarkable observations.

3.5.2 Diode Effects, Circuits and Sensors

Since the first decade of the 2000s, people speak about oxitronics, that is electronic circuits made of oxide systems, taking advantage of the very diverse behaviors of oxide systems.

A radically new approach has been proposed at the very beginning: the conducting circuit could be written by atomic force microscopy on an insulating three-unit-cells-thick LAO/STO interface as described in Sect. 3.4 [86]. Of course this lithography technique is not viable for consumer products, but could be useful for very peculiar applications [70, 77]. It also permits to study clean circuits of variable geometries to investigate size or quantum effects [87], which are interesting from a fundamental point of view.

A more traditional approach has been used to design circuits, starting from diodes [88] to complete oscillator circuits [89] using field effect transistors [90]. Diodes with extremely large blocking voltage can be realized, as well as very large capacitances [35] thanks to the particularities of the LAO/STO system: The 2DES can be completely expelled from below a gate electrode, changing dramatically the effective geometry of the system. These electronic components and circuits are operating at room temperature and above. They might find application in peculiar niche.

Finally, this interface also displays interesting properties as sensor, either of light [91] or of adsorbates, and hence indirectly gas [72].

References

1. S. Thiel, G. Hammerl, A. Schmehl, C. Schneider, J. Mannhart, Tunable quasi-two-dimensional electron gases in oxide heterostructures. Science **313**(5795), 1942–1945 (2006)
2. A.D. Caviglia, S. Gariglio, N. Reyren, D. Jaccard, T. Schneider, M. Gabay, S. Thiel, G. Hammerl, J. Mannhart, J.M. Triscone, Electric field control of the $LaAlO_3/SrTiO_3$ interface ground state. Nature **456**(7222), 624–627 (2008). https://doi.org/10.1038/nature07576
3. C. Bell, S. Harashima, Y. Kozuka, M. Kim, B.G. Kim, Y. Hikita, H. Hwang, Dominant mobility modulation by the electric field effect at the $LaAlO_3/SrTiO_3$ interface. Phy. Rev. Lett. **103**(22), 226802 (2009)
4. A.D. Caviglia, M. Gabay, S. Gariglio, N. Reyren, C. Cancellieri, J.M. Triscone, Tunable rashba spin-orbit interaction at oxide interfaces. Phy. Rev. Lett. **104**(12), 126803 (2010). https://doi.org/10.1103/PhysRevLett.104.126803, http://link.aps.org/doi/10.1103/PhysRevLett.104.126803
5. M. Ben Shalom, M. Sachs, D. Rakhmilevitch, A. Palevski, Y. Dagan, Tuning spin-orbit coupling and superconductivity at the $LaAlO_3/SrTiO_3$ interface: a magnetotransport study. Phy. Rev. Lett. **104**(12), 126802 (2010). https://doi.org/10.1103/PhysRevLett.104.126802, http://link.aps.org/doi/10.1103/PhysRevLett.104.126802
6. A. Fête, S. Gariglio, A. Caviglia, J.M. Triscone, M. Gabaym, Rashba induced magnetoconductance oscillations in the $LaAlO_3/SrTiO_3$ heterostructure. Phy. Rev. B **86**(20), 201105 (2012)
7. A. Caviglia, S. Gariglio, C. Cancellieri, B. Sacepe, A. Fete, N. Reyren, M. Gabay, A. Morpurgo, J.M. Triscone, Two-dimensional quantum oscillations of the conductance at $LaAlO_3/SrTiO_3$ interfaces. Phy. Rev. Lett. **105**(23), 236802 (2010)
8. A. Fête, S. Gariglio, C. Berthod, D. Li, D. Stornaiuolo, M. Gabay, J. Triscone, Large modulation of the shubnikov? de haas oscillations by the rashba interaction at the $LaAlO_3/SrTiO_3$ interface. N. J. Phy. **16**(11), 112002 (2014)
9. M. Diez, A. Monteiro, G. Mattoni, E. Cobanera, T. Hyart, E. Mulazimoglu, N. Bovenzi, C. Beenakker, A. Caviglia, Giant negative magnetoresistance driven by spin-orbit coupling at the $LaAlO_3/SrTiO_3$ interface. Phy. Rev. Lett. **115**(1), 016803 (2015)
10. L. Li, C. Richter, S. Paetel, T. Kopp, J. Mannhart, R. Ashoori, Very large capacitance enhancement in a two-dimensional electron system. Science **332**(6031), 825–828 (2011)
11. M. Rössle, K.W. Kim, A. Dubroka, P. Marsik, C.N. Wang, R. Jany, C. Richter, J. Mannhart, C. Schneider, A. Frano et al., Electric-field-induced polar order and localization of the confined electrons in $LaAlO_3/SrTiO_3$ heterostructures. Phy. Rev. Lett.**110**(13), 136805 (2013)
12. C. Cantoni, J. Gazquez, F. Miletto Granozio, M.P. Oxley, M. Varela, A.R. Lupini, S.J. Pennycook, C. Aruta, U.S. di Uccio, P. Perna et al., Electron transfer and ionic displacements at the origin of the 2d electron gas at the LAO/STO interface: direct measurements with atomic-column spatial resolution. Adv. Mater. **24**(29), 3952–3957 (2012)
13. C. Jia, S. Mi, M. Faley, U. Poppe, J. Schubert, K. Urban, Oxygen octahedron reconstruction in the $SrTiO_3/LaAlO_3$ heterointerfaces investigated using aberration-corrected ultrahigh-resolution transmission electron microscopy. Phy. Rev. B **79**(8), 081405 (2009)
14. M. Honig, J.A. Sulpizio, J. Drori, A. Joshua, E. Zeldov, S. Ilani, Local electrostatic imaging of striped domain order in $LaAlO_3/SrTiO_3$. Nat. Mater. **12**(12), 1112–1118 (2013)
15. B. Kalisky, E.M. Spanton, H. Noad, J.R. Kirtley, K.C. Nowack, C. Bell, H.K. Sato, M. Hosoda, Y. Xie, Y. Hikita et al., Locally enhanced conductivity due to the tetragonal domain structure in $LaAlO_3/SrTiO_3$ heterointerfaces. Nat. Mater. **12**(12), 1091–1095 (2013)
16. I. Pallecchi, M. Codda, E. Galleani d'Agliano, D. Marré, A.D. Caviglia, N. Reyren, S. Gariglio, J.M. Triscone, Seebeck effect in the conducting $LaAlO_3/SrTiO_3$ interface. Phy. Rev. B **81**(8), 085414 (2010). https://doi.org/10.1103/PhysRevB.81.085414
17. I. Pallecchi, F. Telesio, D. Li, A. Fête, S. Gariglio, J.M. Triscone, A. Filippetti, P. Delugas, V. Fiorentini, D. Marré, Giant oscillating thermopower at oxide interfaces. Nat. Commun. **6** (2015)

18. J.S. Kim, S.S.A. Seo, M.F. Chisholm, R. Kremer, H.U. Habermeier, B. Keimer, H.N. Lee, Nonlinear hall effect and multichannel conduction in $LaAlO_3/SrTiO_3$ superlattices. Phy. Rev. B **82**(20), 201,407 (2010)
19. R. Pentcheva, M. Huijben, K. Otte, W.E. Pickett, J. Kleibeuker, J. Huijben, H. Boschker, D. Kockmann, W. Siemons, G. Koster, et al., Parallel electron-hole bilayer conductivity from electronic interface reconstruction. Phy. Rev. Lett. **104**(16), 166804 (2010)
20. M.B. Shalom, A. Ron, A. Palevski, Y. Dagan, Shubnikov–de haas oscillations in $SrTiO_3/LaAlO_3$ interface. Phy. Rev. Lett. **105**(20), 206401 (2010)
21. S. Lerer, M. Ben Shalom, G. Deutscher, Y. Dagan, Low-temperature dependence of the thermomagnetic transport properties of the $SrTiO_3/LaAlO_3$ interface. Phy. Rev. B **84**(7), 075423 (2011). https://doi.org/10.1103/PhysRevB.84.075423, http://link.aps.org/doi/10.1103/PhysRevB.84.075423
22. J. Biscaras, N. Bergeal, S. Hurand, C. Grossetête, A. Rastogi, R. Budhani, D. LeBoeuf, C. Proust, J. Lesueur, Two-dimensional superconducting phase in $LaAlO_3/SrTiO_3$ heterostructures induced by high-mobility carrier doping. Phy. Rev. Lett. **108**(24), 247004 (2012)
23. P. Brinks, W. Siemons, J. Kleibeuker, G. Koster, G. Rijnders, M. Huijben, Anisotropic electrical transport properties of a two-dimensional electron gas at $SrTiO_3$-$LaAlO_3$ interfaces. Appl. Phy. Lett. **98**(24), 242904 (2011)
24. A. Joshua, S. Pecker, J. Ruhman, E. Altman, S. Ilani, A universal critical density underlying the physics of electrons at the $LaAlO_3/SrTiO_3$ interface. Nat. Commun. **3**, 1129 (2012)
25. M.B. Shalom, C. Tai, Y. Lereah, M. Sachs, E. Levy, D. Rakhmilevitch, A. Palevski, Y. Dagan, Anisotropic magnetotransport at the $SrTiO_3/LaAlO_3$ interface. Physical Review B **80**(14), 140403 (2009)
26. A. Annadi, Z. Huang, K. Gopinadhan, X.R. Wang, A. Srivastava, Z. Liu, H.H. Ma, T. Sarkar, T. Venkatesan et al., Fourfold oscillation in anisotropic magnetoresistance and planar hall effect at the $LaAlO_3/SrTiO_3$ heterointerfaces: effect of carrier confinement and electric field on magnetic interactions. Phys. Rev. B **87**(20), 201102 (2013)
27. Y. Liao, T. Kopp, C. Richter, A. Rosch, J. Mannhart, Metal-insulator transition of the $LaAlO_3/SrTiO_3$ interface electron system. Phy. Rev. B **83**(7), 075402 (2011)
28. C. Cancellieri, M.L. Reinle-Schmitt, M. Kobayashi, V.N. Strocov, P. Willmott, D. Fontaine, P. Ghosez, A. Filippetti, P. Delugas, V. Fiorentini, Doping-dependent band structure of $LaAlO_3/SrTiO_3$ interfaces by soft x-ray polarization-controlled resonant angle-resolved photoemission. Phy. Rev. B **89**(12), 121412 (2014)
29. J. Ruhman, A. Joshua, S. Ilani, E. Altman, Competition between kondo screening and magnetism at the $LaAlO_3/SrTiO_3$ interface. Phy. Rev. B **90**(12), 125123 (2014)
30. M.H. Fischer, S. Raghu, E.A. Kim, Spin–orbit coupling in $LaAlO_3/SrTiO_3$ interfaces: magnetism and orbital ordering. N. J. Phy. **15**(2), 023022 (2013)
31. Y. Kim, R.M. Lutchyn, C. Nayak, Origin and transport signatures of spin-orbit interactions in one-and two-dimensional $SrTiO_3$-based heterostructures. Phy. Rev. B **87**(24), 245,121 (2013)
32. A. Brinkman, M. Huijben, M. van Zalk, J. Huijben, U. Zeitler, J.C. Maan, W.G. van der Wiel, G. Rijnders, D.H.A. Blank, H. Hilgenkamp, Magnetic effects at the interface between non-magnetic oxides. Nat. Mater. **6**(7), 493–496 (2007). https://doi.org/10.1038/nmat1931, http://www.nature.com/doifinder/10.1038/nmat1931
33. N. Reyren, S. Thiel, A.D. Caviglia, L.F. Kourkoutis, G. Hammerl, C. Richter, C.W. Schneider, T. Kopp, A.S. Ruetschi, D. Jaccard, M. Gabay, D.A. Muller, J.M. Triscone, J. Mannhart, Superconducting interfaces between insulating oxides. Science **317**(5842), 1196–1199 (2007). https://doi.org/10.1126/science.1146006, http://www.sciencemag.org/cgi/doi/10.1126/science.1146006
34. N. Reyren, S. Gariglio, A.D. Caviglia, D. Jaccard, T. Schneider, J.M. Triscone, Anisotropy of the superconducting transport properties of the $LaAlO_3/SrTiO_3$ interface. Appl. Phy. Lett. **94**(11), 112506 (2009). https://doi.org/10.1063/1.3100777, http://scitation.aip.org/content/aip/journal/apl/94/11/10.1063/1.3100777
35. L. Li, C. Richter, J. Mannhart, R.C. Ashoori, Coexistence of magnetic order and two-dimensional superconductivity at $LaAlO_3/SrTiO_3$ interfaces. Nat. Phy. **7**(10), 762–766 (2011). https://doi.org/10.1038/nphys2080, http://www.nature.com/doifinder/10.1038/nphys2080

36. A.P. Petrović, A. Paré, T.R. Paudel, K. Lee, S. Holmes, C.H.W. Barnes, A. David, T. Wu, E.Y. Tsymbal, C. Panagopoulos, Emergent vortices at a ferromagnetic superconducting oxide interface. N. J. Phy. **16**(10), 103012 (2014). https://doi.org/10.1088/1367-2630/16/10/103012, http://stacks.iop.org/1367-2630/16/i=10/a=103012?key=crossref.95d78e23175af9dfd7f98da58155c926
37. J.A. Bert, B. Kalisky, C. Bell, M. Kim, Y. Hikita, H.Y. Hwang, K.A. Moler, Direct imaging of the coexistence of ferromagnetism and superconductivity at the $LaAlO_3/SrTiO_3$ interface. Nat. Phy. **7**(10), 767–771 (2011). https://doi.org/10.1038/nphys2079, http://www.nature.com/doifinder/10.1038/nphys2079
38. D.A. Dikin, M. Mehta, C.W. Bark, C.M. Folkman, C.B. Eom, V. Chandrasekhar, Coexistence of superconductivity and ferromagnetism in two dimensions. Phy. Rev. Lett. **107**(5), 056802 (2011). https://doi.org/10.1103/PhysRevLett.107.056802, http://link.aps.org/doi/10.1103/PhysRevLett.107.056802
39. M.P. Warusawithana, C. Richter, J.A. Mundy, P. Roy, J. Ludwig, S. Paetel, T. Heeg, A.A. Pawlicki, L.F. Kourkoutis, M. Zheng, M. Lee, B. Mulcahy, W. Zander, Y. Zhu, J. Schubert, J.N. Eckstein, D.A. Muller, C.S. Hellberg, J. Mannhart, D.G. Schlom, LaAlO3 stoichiometry is key to electron liquid formation at $LaAlO_3/SrTiO_3$ interfaces. Nat. Commun. **4**, 2351 (2013). https://doi.org/10.1038/ncomms3351
40. K. Narayanapillai, K. Gopinadhan, X. Qiu, A. Annadi, Ariando, T. Venkatesan, H. Yang, Current-driven spin orbit field in $LaAlO_3/SrTiO_3$ heterostructures. Appl. Phy. Lett. **105**(16), 162405 (2014). https://doi.org/10.1063/1.4899122
41. Ariando, X. Wang, G. Baskaran, Z.Q. Liu, J. Huijben, J.B. Yi, A. Annadi, A.R. Barman, A. Rusydi, S. Dhar, Y.P. Feng, J. Ding, H. Hilgenkamp, T. Venkatesan, Electronic phase separation at the $LaAlO_3/SrTiO_3$ interface. Nat. Commun. **2**, 188 (2011). https://doi.org/10.1038/ncomms1192, http://www.nature.com/doifinder/10.1038/ncomms1192
42. N. Pavlenko, T. Kopp, E.Y. Tsymbal, G.A. Sawatzky, J. Mannhart, Magnetic and superconducting phases at the $LaAlO_3/SrTiO_3$ interface: the role of interfacial Ti 3*d* electrons. Phy. Rev. B **85**(2), 020407 (2012). https://doi.org/10.1103/PhysRevB.85.020407, http://link.aps.org/doi/10.1103/PhysRevB.85.020407
43. L. Weston, X.Y. Cui, S.P. Ringer, C. Stampfl, Density-functional prediction of a surface magnetic phase in $LaAlO_3/SrTiO_3$ heterostructures induced by Al vacancies. Phy. Rev. Lett. **113**(18), 186401 (2014). https://doi.org/10.1103/PhysRevLett.113.186401, http://link.aps.org/doi/10.1103/PhysRevLett.113.186401
44. J.S. Lee, Y.W. Xie, H.K. Sato, C. Bell, Y. Hikita, H.Y. Hwang, C.C. Kao, Titanium dxy ferromagnetism at the $LaAlO_3/SrTiO_3$ interface. Nature Materials **12**(8), 703–706 (2013). https://doi.org/10.1038/nmat3674, http://www.nature.com/doifinder/10.1038/nmat3674
45. M.R. Fitzsimmons, N.W. Hengartner, S. Singh, M. Zhernenkov, F.Y. Bruno, J. Santamaria, A. Brinkman, M. Huijben, H.J.A. Molegraaf, J. de la Venta, I.K. Schuller, Upper limit to magnetism in $LaAlO_3/SrTiO_3$ heterostructures. Phy. Rev. Lett. **107**(21), 217201 (2011). https://doi.org/10.1103/PhysRevLett.107.217201, http://link.aps.org/doi/10.1103/PhysRevLett.107.217201
46. E. Lesne, N. Reyren, D. Doennig, R. Mattana, H. Jaffrès, V. Cros, F. Petroff, F. Choueikani, P. Ohresser, R. Pentcheva, A. Barthélémy, M. Bibes, Suppression of the critical thickness threshold for conductivity at the $LaAlO_3/SrTiO_3$ interface. Nat. Commun. **5** (2014). https://doi.org/10.1038/ncomms5291, http://www.nature.com/doifinder/10.1038/ncomms5291
47. M. Salluzzo, S. Gariglio, D. Stornaiuolo, V. Sessi, S. Rusponi, C. Piamonteze, G.M. De Luca, M. Minola, D. Marré, A. Gadaleta, H. Brune, F. Nolting, N.B. Brookes, G. Ghiringhelli, Origin of interface magnetism in $BiMnO_3/SrTiO_3$ and $LaAlO_3/SrTiO_3$ heterostructures. Phy. Rev. Lett. **111**(8), 087204 (2013). https://doi.org/10.1103/PhysRevLett.111.087204, http://link.aps.org/doi/10.1103/PhysRevLett.111.087204
48. B. Kalisky, J.A. Bert, C. Bell, Y. Xie, H.K. Sato, M. Hosoda, Y. Hikita, H.Y. Hwang, K.A. Moler, Scanning probe manipulation of magnetism at the $LaAlO_3/SrTiO_3$ heterointerface. Nano Lett. **12**(8), 4055–4059 (2012). https://doi.org/10.1021/nl301451e, http://pubs.acs.org/doi/abs/10.1021/nl301451e

49. F. Bi, M. Huang, H. Lee, C.B. Eom, P. Irvin, J. Levy, $LaAlO_3$ thickness window for electronically controlled magnetism at $LaAlO_3/SrTiO_3$ heterointerfaces. Appl. Phy. Lett. **107**(8), 082402 (2015). https://doi.org/10.1063/1.4929430, http://scitation.aip.org/content/aip/journal/apl/107/8/10.1063/1.4929430
50. T.D. Ngo, J.W. Chang, K. Lee, S. Han, J.S. Lee, Y.H. Kim, M.H. Jung, Y.J. Doh, M.S. Choi, J. Song, J. Kim, Polarity-tunable magnetic tunnel junctions based on ferromagnetism at oxide heterointerfaces. Nat. Commun. **6**, 8035 (2015). https://doi.org/10.1038/ncomms9035, http://www.nature.com/doifinder/10.1038/ncomms9035
51. M. Honig, J.A. Sulpizio, J. Drori, A. Joshua, E. Zeldov, S. Ilani, Local electrostatic imaging of striped domain order in $LaAlO_3/SrTiO_3$. Nat. Mater. **12**(12), 1112–1118 (2013). https://doi.org/10.1038/nmat3810, http://www.nature.com/doifinder/10.1038/nmat3810
52. S. Banerjee, O. Erten, M. Randeria, Ferromagnetic exchange, spinorbit coupling and spiral magnetism at the $LaAlO_3/SrTiO_3$ interface. Nat. Phy. **9**(10), 626–630 (2013). https://doi.org/10.1038/nphys2702, http://www.nature.com/doifinder/10.1038/nphys2702
53. C.S. Koonce, M.L. Cohen, J.F. Schooley, W.R. Hosler, E.R. Pfeiffer, Superconducting transition temperatures of semiconducting $SrTiO_3$. Phy. Rev. **163**(2), 380–390 (1967). https://doi.org/10.1103/PhysRev.163.380
54. J.F. Schooley, W.R. Hosler, M.L. Cohen, Superconductivity in Semiconducting $SrTiO_3$. Physical Review Letters **12**(17), 474–475 (1964). https://doi.org/10.1103/PhysRevLett.12.474, http://link.aps.org/doi/10.1103/PhysRevLett.12.474
55. E.R. Pfeiffer, J.F. Schooley, Superconducting transition temperature of Nb-doped $SrTiO_3$. Phy. Lett. **29A**(10), 589–590 (1969)
56. Y. Kozuka, M. Kim, C. Bell, B.G. Kim, Y. Hikita, H.Y. Hwang, Two-dimensional normal-state quantum oscillations in a superconducting heterostructure. Nature **462**(7272), 487–490 (2009). https://doi.org/10.1038/nature08566
57. J. Nishimura, A. Ohtomo, A. Ohkubo, Y. Murakami, M. Kawasaki, Controlled carrier generation at a polarity-discontinued perovskite heterointerface. Jpn. J. Appl. Phy. **43**(8A), L1032–L1034 (2004). https://doi.org/10.1143/JJAP.43.L1032, http://stacks.iop.org/1347-4065/43/L1032
58. G. Binnig, A. Baratoff, H.E. Hoenig, J.G. Bednorz, Two-band Superconductivity in Nb-Doped $SrTiO_3$. Phys. Rev. Lett. **45**(15), 1352–1355 (1980)
59. C. Richter, H. Boschker, W. Dietsche, E. Fillis-Tsirakis, R. Jany, F. Loder, L.F. Kourkoutis, D.A. Muller, J.R. Kirtley, C.W. Schneider, J. Mannhart, Interface superconductor with gap behaviour like a high-temperature superconductor. Nature **502**(7472), 528–531 (2013). https://doi.org/10.1038/nature12494
60. H. Boschker, C. Richter, E. Fillis-Tsirakis, C.W. Schneider, J. Mannhart, Electronphonon coupling and the superconducting phase diagram of the $LaAlO_3$-$SrTiO_3$ interface. Sci. Rep. **5**(12309) (2015). https://doi.org/10.1038/srep12309
61. G.N. Daptary, S. Kumar, P. Kumar, A. Dogra, N. Mohanta, A. Taraphder, A. Bid, Correlated non-Gaussian phase fluctuations in $LaAlO_3/SrTiO_3$ heterointerfaces. Phy. Rev. B **94**(8), 085104 (2016). https://doi.org/10.1103/PhysRevB.94.085104, http://link.aps.org/doi/10.1103/PhysRevB.94.085104
62. T. Schneider, S. Weyeneth, Suppression of the Berezinskii-Kosterlitz-Thouless and quantum phase transitions in two-dimensional superconductors by finite-size effects. Phy. Rev. B **90**(6), 064501 (2014). https://doi.org/10.1103/PhysRevB.90.064501, http://link.aps.org/doi/10.1103/PhysRevB.90.064501
63. B.S. Chandrasekhar, A note on the maximum critical field of high field superconductors. Appl. Phy. Lett. **1**(1), 7–8 (1962)
64. A.M. Clogston, Upper limit for the critical field in hard superconductors. Phy. Rev. Lett. **9**(6), 266–267 (1962). https://doi.org/10.1103/PhysRevLett.9.266, http://link.aps.org/doi/10.1103/PhysRevLett.9.266
65. K. Michaeli, A.C. Potter, P.A. Lee, Superconducting and ferromagnetic phases in $LaAlO_3/SrTiO_3$ oxide interface structures: possibility of finite momentum pairing. Phy. Rev. Lett. **108**(11), 117003 (2012). https://doi.org/10.1103/PhysRevLett.108.117003, http://link.aps.org/doi/10.1103/PhysRevLett.108.117003

66. S. Gariglio, M. Gabay, J.M. Triscone, Research update: conductivity and beyond at the $LaAlO_3/SrTiO_3$ interface. APL Mater. **4**(6), 060701 (2016). https://doi.org/10.1063/1.4953822
67. S. Hurand, A. Jouan, C. Feuillet-Palma, G. Singh, J. Biscaras, E. Lesne, N. Reyren, A. Barthélémy, M. Bibes, J.E. Villegas, C. Ulysse, X. Lafosse, M. Pannetier-Lecoeur, S. Caprara, M. Grilli, J. Lesueur, N. Bergeal, Field-effect control of superconductivity and Rashba spin-orbit coupling in top-gated $LaAlO_3/SrTiO_3$ devices. Sci. Rep. **5**(12751) (2015). https://doi.org/10.1038/srep12751
68. P.D. Eerkes, W.G. van der Wiel, H. Hilgenkamp, Modulation of conductance and superconductivity by top-gating in $LaAlO_3/SrTiO_3$ 2-dimensional electron systems. Appl. Phy. Lett. **103**(20), 201603 (2013). https://doi.org/10.1063/1.4829555, http://scitation.aip.org/content/aip/journal/apl/103/20/10.1063/1.4829555
69. M. Hosoda, Y. Hikita, H.Y. Hwang, C. Bell: Transistor operation and mobility enhancement in top-gated $LaAlO_3/SrTiO_3$ heterostructures. Appl. Phy. Lett. **103**(10), 103507 (2013). https://doi.org/10.1063/1.4820449, http://scitation.aip.org/content/aip/journal/apl/103/10/10.1063/1.4820449
70. G. Cheng, P.F. Siles, F. Bi, C. Cen, D.F. Bogorin, C.W. Bark, C.M. Folkman, J.W. Park, C.B. Eom, G. Medeiros-Ribeiro, J. Levy, Sketched oxide single-electron transistor. Nat. Nanotechnol. **6**(6), 343–347 (2011). https://doi.org/10.1038/nnano.2011.56, http://www.nature.com/doifinder/10.1038/nnano.2011.56
71. D. Stornaiuolo, S. Gariglio, A. Fête, M. Gabay, D. Li, D. Massarotti, J.M. Triscone, Weak localization and spin-orbit interaction in side-gate field effect devices at the $LaAlO_3/SrTiO_3$ interface. Phy. Rev. B **90**(23), 235426 (2014). https://doi.org/10.1103/PhysRevB.90.235426, http://link.aps.org/doi/10.1103/PhysRevB.90.235426
72. Y. Xie, Y. Hikita, C. Bell, H.Y. Hwang, Control of electronic conduction at an oxide heterointerface using surface polar adsorbates. Nat. Commun. **2**, 494 (2011). https://doi.org/10.1038/ncomms1501
73. J. Biscaras, S. Hurand, C. Feuillet-Palma, A. Rastogi, R.C. Budhani, N. Reyren, E. Lesne, J. Lesueur, N. Bergeal, Limit of the electrostatic doping in two-dimensional electron gases of $LaXO_3(X = Al, Ti)/SrTiO_3$. Sci. Rep. **4**, 6788 (2014). https://doi.org/10.1038/srep06788
74. Z. Liu, C. Li, W. Lü, X. Huang, Z. Huang, S. Zeng, X. Qiu, L. Huang, A. Annadi, J. Chen et al., Origin of the two-dimensional electron gas at $laalo_3/srtio_3$ interfaces: the role of oxygen vacancies and electronic reconstruction. Phy. Rev. X **3**(2), 021010 (2013)
75. C.W. Schneider, S. Thiel, G. Hammerl, C. Richter, J. Mannhart, Microlithography of electron gases formed at interfaces in oxide heterostructures. Appl. Phy. Lett. **89**(12), 122101–122101 (2006)
76. D. Stornaiuolo, S. Gariglio, N. Couto, A. Fete, A. Caviglia, G. Seyfarth, D. Jaccard, A. Morpurgo, J.M. Triscone, In-plane electronic confinement in superconducting $LaAlO_3/SrTiO_3$ nanostructures. Appl. Phy. Lett. **101**(22), 222601 (2012)
77. C. Cen, S. Thiel, J. Mannhart, J. Levy, Oxide Nanoelectronics on Demand. Science **323**(5917), 1026–1030 (2009). https://doi.org/10.1126/science.1168294
78. C. Cen, S. Thiel, G. Hammerl, C. Schneider, K. Andersen, C. Hellberg, J. Mannhart, J. Levy, Nanoscale control of an interfacial metal-insulator transition at room temperature. Nat. Mater. **7**(4), 298–302 (2008)
79. Y. Xie, C. Bell, Y. Hikita, H.Y. Hwang, Tuning the electron gas at an oxide heterointerface via free surface charges. Adv. Mater. **23**(15), 1744–1747 (2011)
80. F. Bi, D.F. Bogorin, C. Cen, C.W. Bark, J.W. Park, C.B. Eom, J. Levy, "water-cycle" mechanism for writing and erasing nanostructures at the $LaAlO_3/SrTiO_3$ interface. Appl. Phy. Lett. **97**, 173110 (2010)
81. N. Reyren, M. Bibes, E. Lesne, J.M. George, C. Deranlot, S. Collin, A. Barthélémy, H. Jaffrès, Gate-controlled spin injection at $LaAlO_3/SrTiO_3$ interfaces. Phy. Rev. Lett. **108**(18), 186802 (2012). https://doi.org/10.1103/PhysRevLett.108.186802, http://link.aps.org/doi/10.1103/PhysRevLett.108.186802

82. A.G. Swartz, S. Harashima, Y. Xie, D. Lu, B. Kim, C. Bell, Y. Hikita, H.Y. Hwang, Spin-dependent transport across Co/$LaAlO_3$/$SrTiO_3$ heterojunctions. Appl. Phy. Lett. **105**(3), 032406 (2014). https://doi.org/10.1063/1.4891174, http://scitation.aip.org/content/aip/journal/apl/105/3/10.1063/1.4891174
83. W. Han, X. Jiang, A. Kajdos, S.h. Yang, S. Stemmer, S.S.P. Parkin, Spin injection and detection in lanthanum- and niobium-doped $SrTiO_3$ using the Hanle technique. Nat. Commun. **4**, 1–6 (2013). https://doi.org/10.1038/ncomms3134
84. A.M. Kamerbeek, E.K. de Vries, A. Dankert, S.P. Dash, B.J. van Wees, T. Banerjee, Electric field effects on spin accumulation in Nb-doped $SrTiO_3$ using tunable spin injection contacts at room temperature. Appl. Phy. Lett. **104**(21), 212106 (2014). https://doi.org/10.1063/1.4880895, http://scitation.aip.org/content/aip/journal/apl/104/21/10.1063/1.4880895
85. E. Lesne, Y. Fu, S. Oyarzun, J.C. Rojas-Sanchez, D.C. Vaz, H. Naganuma, G. Sicoli, J.P. Attané, M. Jamet, E. Jacquet, J.M. George, A. Bathélémy, H. Jaffrès, A. Fert, M. Bibes, L. Vila, Highly efficient and tunable spin-to-charge conversion through Rashba coupling at oxide interfaces. Nat. Mater. **15**, 1261 (2016). https://doi.org/10.1038/NMAT4726
86. C. Cen, S. Thiel, G. Hammerl, C.W. Schneider, K.E. Andersen, C.S. Hellberg, J. Mannhart, J. Levy, Nanoscale control of an interfacial metalinsulator transition at room temperature. Nat. Mater. **7**(4), 298–302 (2008). https://doi.org/10.1038/nmat2136, http://www.nature.com/doifinder/10.1038/nmat2136
87. D. Stornaiuolo, S. Gariglio, N.J.G. Couto, A. Fete, A.D. Caviglia, G. Seyfarth, D. Jaccard, A.F. Morpurgo, J.M. Triscone, In-plane electronic confinement in superconducting $LaAlO_3$/$SrTiO_3$ nanostructures. Appl. Phy. Lett. **101**(22), 222601 (2012). https://doi.org/10.1063/1.4768936, http://scitation.aip.org/content/aip/journal/apl/101/22/10.1063/1.4768936
88. B. Forg, C. Richter, J. Mannhart, Field-effect devices utilizing $LaAlO_3$/$SrTiO_3$ interfaces. Appl. Phys. Lett. **100**(5), 053506 (2012). https://doi.org/10.1063/1.3682102, http://scitation.aip.org/content/aip/journal/apl/100/5/10.1063/1.3682102
89. R. Jany, C. Richter, C. Woltmann, G. Pfanzelt, B. Förg, M. Rommel, T. Reindl, U. Waizmann, J. Weis, J.A. Mundy, D.A. Muller, H. Boschker, J. Mannhart, Monolithically integrated circuits from functional oxides. Adv. Mater. Interfaces **1**(1), 1300031 (2014). https://doi.org/10.1002/admi.201300031, http://doi.wiley.com/10.1002/admi.201300031
90. C. Woltmann, T. Harada, H. Boschker, V. Srot, P.A. van Aken, H. Klauk, J. Mannhart, Field-effect transistors with submicrometer gate lengths fabricated from $LaAlO_3$-$SrTiO_3$-based heterostructures. Phy. Rev. Appl. **4**(6), 064003 (2015). https://doi.org/10.1103/PhysRevApplied.4.064003, http://link.aps.org/doi/10.1103/PhysRevApplied.4.064003
91. A. Tebano, E. Fabbri, D. Pergolesi, G. Balestrino, E. Traversa, Room-temperature in $SrTiO_3$/$LaAlO_3$ heterostructures. ACS Nano **6**(2), 1278–1283 (2012). https://doi.org/10.1021/nn203991q